33RD INTERNATIONAL COSMIC RAY CONFERENCE, RIO DE JANEIRO 2013
THE ASTROPARTICLE PHYSICS CONFERENCE

ICRC 2013

Cosmic Ray Muon Forbush Decrease Caused by Magnetic Clouds from 2009 to 2011

ROCKENBACH, M.[1], ECHER, E.[2], DAL LAGO, A.[2], BRAGA, C.R.[2], MENDONA, R.R.S.[2], OLIVEIRA, A.G.[1], SCHUCH, N.J.[3], KUWABARA, T.[4], MUNAKATA, K.[5]

[1] *Universidade do Vale do Paraíba, São José dos Campos, Brazil*
[2] *Space Geophysics Department, National Institute for Space Research, São José dos Campos, Brazil*
[3] *Southern Space Research Center - National Institute of Space Research, in collaboration with Space Science Laboratory of Santa Maria, Santa Maria, Brazil*
[4] *Bartol Research Institute and Department of Physics and Astronomy, University of Delaware, Newark, DE 19716, USA*
[5] *Physics Department, Faculty of Science, Shinshu University, Matsumoto, Japan.*

marlosrs@gmail.com

Abstract: We have a preliminary investigation of the cosmic ray decreases caused by magnetic clouds (MCs). The cosmic ray density, separated from the anisotropy, was calculated using the 12 hours trailing moving average of the best-fit parameters of the Global Muon Detector Network (GMDN) data. The properties of the Interplanetary Magnetic Field (IMF) and the solar wind were compared with cosmic ray density and anisotropy vector during the MCs structures from 2009 to 2011, in order to study the Forbush decrease, observed in cosmic ray data, caused by these solar structures. We will describe the two events that had the biggest cosmic ray decrease detailed.

Keywords: Muon, Forbush Decrease, Magnetic Clouds, Solar Structures

1 Introduction

Interplanetary Coronal Mass Ejections (ICMEs) are solar plasma structures ejected from the Sun, and can eventually hit the Earth, and cause geomagnetic storms. The geomagnetic storms are associated with MCs and sheath field following interplanetary shocks, although they frequently involve consecutive and complex ICME structures [1]. [2] was first to observe a decrease of a few percent in the cosmic ray count rate during geomagnetic storms. Some years latter [3] showed that the cosmic ray decreases are caused by corotating high-speed streams: for recurrent decreases, and for non-recurrent decreases, are caused by transient solar wind structures associated with ICMEs. Many authors have studied the relationship between cosmic rays and ICME [10, 9, 14, 11, 13]. All those authors correlates the ICMEs with neutron monitor data. In this paper we correlate ICMEs with cosmic ray muon data from the GMDN to find the contribution of the magnetic cloud on the Forbush decrease.

2 Data and Methodology

2.1 Ground Muon Detector Network (GMDN) Data

The GMDN are a muon detector network composed by three scintillators located in: Nagoya, Japan; Hobart, Australia and São Martinho da Serra, Brazil and one hodoscope installed in Kuwait City, Kuwait. These detectors can register the cosmic ray count rate in 60 directional channels simultaneously.

It is possible to derive the GCR density in the interplanetary medium separated from the anisotropy vector components using the coupling coefficients [4] of the GCR throughout the atmosphere. We fit the value of the percentual variation of the hourly counting rate recorded by the j-th channel of the i-th detector of the GMDN, $I_{i,j}^{obs}$, after remove the barometric effect. The best-fit equation is:

$$\begin{aligned} \bar{I}_{i,j}^{fit} &= \bar{I}^0(t) + \bar{\xi}_x^{GEO}(t)(c_{1i,j}^1 cos\omega.t_i - s_{1i,j}^1 sin\omega.t_i) \\ &+ \bar{\xi}_y^{GEO}(t)(s_{1i,j}^1 cos\omega.t_i - c_{1i,j}^1 sin\omega.t_i) \\ &+ \bar{\xi}_z^{GEO}(t) c_{1i,j}^0 \end{aligned} \quad (1)$$

where $c_{1i,j}^1$, $s_{1i,j}^1$ and $c_{1i,j}^0$ are the coupling coefficients determined assuming a rigidity independent of the anisotropy [4], t is the universal time, $\omega = \pi/12$, t_i is the local time of i-th detector. $\bar{I}^0$, $\bar{\xi}_x^{GEO}$, $\bar{\xi}_y^{GEO}$ and $\bar{\xi}_z^{GEO}$ are the fitted parameters calculated from the 12 hours trailing moving average [5]. The anisotropy vector components are: $\bar{\xi}_x^{GEO}$, $\bar{\xi}_y^{GEO}$ and $\bar{\xi}_z^{GEO}$; and the cosmic ray density is $\bar{I}^0$. The GMDN data were obtained from the Bartol Research Institute (`ftp://ftp.bartol.udel.edu/takao/muon_data/`).

2.2 ICME Ace Data

MCs are a subset of the ICMEs, and can be identified using three criteria: (1) large-scale smooth field rotation; (2) enhanced magnetic field magnitude. and (3) low plasma temperature and plasma beta [15, 16]. Solar wind data were obtained from ACE satellite plasma and magnetic field instruments (`www.srl.caltech.edu/ACE/`).

3 Results and Discussions

We chose solar MCs occurred between 2009 to 2011, when the GMDN was in full operation. This period corresponds to the rising phase of the solar cycle 24. During this period, 18 MCs were selected from the ICME list published in [12]. All structures analyzed are shown in Table 1.

Table 2 summarize parameter found the peak value of IMF intensity $|B|_p$(nT), the maximum Solar Wind speed V_p(km/s), and the GMDN cosmic ray density decrease $\Delta I(\%)$, from ACE satellite, and GMDN data.

Table 1: Magnetic clouds start and end times, identified by [12].

Magnetic Cloud		
	Start	End
08-MC1	Dec 17, 2008 - 0300h	Dec 17, 2008 - 1400h
09-MC1	Feb 04, 2009 - 0000h	Feb 04, 2009 - 1600h
09-MC2	Oct 29, 2009 - 0500h	Oct 29, 2009 - 2300h
10-MC1	Feb 07, 2010 - 1800h	Feb 08, 2010 - 2200h
10-MC2	Apr 05, 2010 - 1200h	Apr 06, 2010 - 1400h
10-MC3	Apr 12, 2010 - 0100h	Apr 12, 2010 - 1500h
10-MC4	May 28, 2010 - 1900h	May 29, 2010 - 1700h
10-MC5	Aug 04, 2010 - 1000h	Aug 05, 2010 - 0000h
10-MC6	Dec 28, 2010 - 0300h	Dec 28, 2010 - 1500h
11-MC1	Feb 04, 2011 - 1300h	Feb 04, 2011 - 2000h
11-MC2	Mar 29, 2011 - 2300h	Mar 31, 2011 - 0400h
11-MC3	May 28, 2011 - 0500h	May 28, 2011 - 2100h
11-MC4	Sep 10, 2011 - 0300h	Sep 10, 2011 - 1500h
11-MC5	Sep 17, 2011 - 1400h	Sep 18, 2011 - 0600h
11-MC6	Oct 06, 2011 - 1200h	Oct 06, 2011 - 2300h
11-MC7	Oct 24, 2011 - 2200h	Oct 25, 2011 - 1600h
11-MC8	Nov 07, 2011 - 1700h	Nov 07, 2011 - 2300h
11-MC9	Nov 29, 2011- 0000h	Nov 29, 2011- 0800h

Table 2: Parameters obtained from ACE data, and GMDN cosmic ray density. We have the peak value of IMF intensity $|B|_p$, the maximum solar wind speed V_p, and the cosmic ray density decrease ΔI.

	$\|B\|_p$(nT)	V_p(km/s)	$\Delta I(\%)$
08-MC1	9.6	373.2	0.64
09-MC1	11.0	382.9	0.32
09-MC2	11.1	381.8	0.48
10-MC1	10.5	403.5	0.76
10-MC2	19.7	794.8	0.61
10-MC3	11.9	454.9	0.46
10-MC4	14.3	390.9	0.73
10-MC5	17.1	589.3	0.94
10-MC6	13.8	407.2	0.31
11-MC1	21.0	636.2	0.64
11-MC2	14.5	391.4	1.14
11-MC3	13.0	767.4	0.61
11-MC4	20.4	559.2	1.18
11-MC5	14.1	543.7	1.05
11-MC6	12.0	403.6	-
11-MC7	24.5	503.0	1.54
11-MC8	9.9	364.1	0.15
11-MC9	17.1	499.4	0.68

We compared those MCs selected with the Cosmic ray density ($\bar{I}^0$), and the anisotropy components vector ($\bar{\xi}_x^{GEO}$, $\bar{\xi}_y^{GEO}$ and $\bar{\xi}_z^{GEO}$), from the Equation (1). Figures 1 and 2, show two examples of the analyzed structures. From top to bottom we have the IMF intensity, the IMF components x and y, IMF z component, solar wind speed, density, and temperature, plasma beta, GMDN cosmic ray density, three components of the anisotropy, and the bubble plot of pitch angle distribution, that can show same cosmic ray precursor of geomagnetic storms [5].

Figure 3 shows the spectral coherence analysis, that is the cross correlation mean [17], between the IMF intensity and GMDN cosmic ray density and Figure 4 shows the same analysis between the solar wind speed and cosmic ray density, during the period of 11-MC4.

The spectral coherence analysis between IMF intensity and cosmic ray density (Figure 3) shows statistical coherence higher than 95% just durind the MC occurence between doy 253 and 253.5. It corresponds a periodicity of 12 hours (0.25 times of the total duration of the 48 hours). The black arrows indicate the angle phase between those two time series that are in phase, because the arrows have a zero angle to the horizontal and they are pointing to the right [17]. The spectral coherence analysis between solar wind speed and cosmic ray density (Figure 4) do not show any statistical coherence within the 95% limit.

The spectral coherence analysis between IMF intensity and cosmic ray density (Figure 5), and between solar wind speed and cosmic ray density (Figure 6) shows statistical coherence within the 95% limit between doy 297.5 and 298, coincident with the turbulent region between the shock front. It corresponds a periodicity between 6 and 12 hours (0.125 and 0.25 times of the total duration of the 48 hours). In both cases the black arrows indicates that the time series have a non-linear relation, because the arrows have a non-zero angle to the horizontal [17].

4 Conclusions

During the analysed period, we do not have high intense structures, the average of IMF intensity was $|\bar{B}|_p = 14.7$nT, and the Solar Wind speed mean was $\bar{V}_p = 491.5$km/s, that is similar those during quite periods. The average of the cosmic ray density decrease was $\Delta\bar{I} = 0.73(\%)$. In the 2011-MC6 we do not see any cosmic ray decrease. The highest cosmic ray decrease was $\Delta I = 1.54(\%)$ of the 11-MC7. The Forbush decrease is coincidente with the MC structure, that is identified by the vertical black lines in Figure 2. The spectral coherence in the Figures 5 and 6, showed that the highest statistical coherence coincides with the turbulent region between the shock front and the MC. It means that in the turbulent region, both IMF and solar wind speed are important to the cosmic ray modulation.

The second highest cosmic ray decrease was $\Delta I = 1.18(\%)$ of the 11-MC4. The Forbush decrease is also coincidente with the MC structure, between the vertical black lines in Figure 1. The spectral coherence in the Figure 3 showed that the highest statistical coherence coincides with the MC and the Figure 4 do not show any important coherence. It means that the magnetic field is more important to the cosmic ray modulation inside the magnetic cloud, and the solar wind speed do not play any important role.

We need more data to make a better statistics between the IMF, Solar Wind plasma parameters ans the cosmic ray density ans anisotropy.

Acknowledgment: The authors want to thanks FAPESP and CNPq, for financial support under the projects 2011/11581-9 and 300300/2012-3; for National Science Foundation (NFS) of the USA for a subcontract between Delaware University and FATEC/UFSM from Brazil, for supporting part of the upgrade of the telescope installed in São Martinho da Serra, Brazil; for Bartol Research Institute, USA, and Shinshu University for the GMDN data. A. D. Lago thanks CNPq for grants 305351/2011-7 and 481368/2010-8. We thank the ACE MAG and SWEPAM instrument teams and the ACE Science Center for providing the ACE data.

References

[1] W.D. Gonzalez, E. Echer, B.T. Tsurutani, A.L. Cla de Gonzalez and A. Dal Lago,Space Science Reviews, Volume 158, Issue 1, pp.69-89 (2011), doi:10.1007/s11214-010-9715-2.

[2] S.E. Forbush, Phys. Rev. 51, 11081109 (1937), doi:10.1103/PhysRev.51.1108.3.

[3] J.A. Simpson, Physical Review, vol. 94, Issue 2, pp. 426-440 (1954), doi:10.1103/PhysRev.94.426

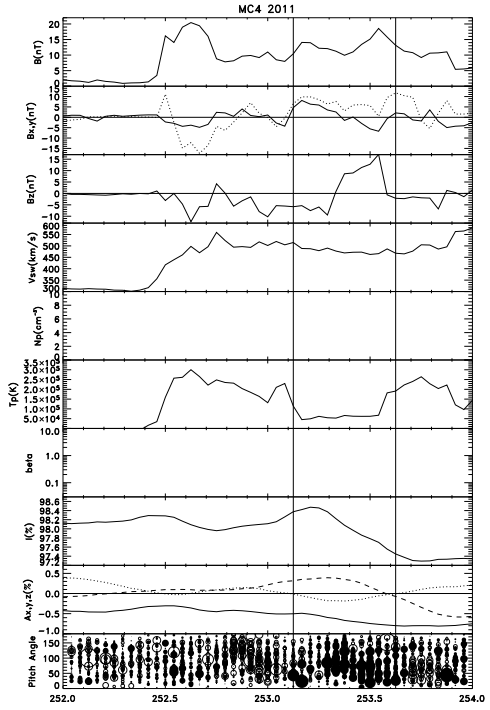

Fig. 1: Magnetic cloud occurred in September 10, 2011. From top to bottom we have the IMF intensity, the IMF components x and y, IMF z component, solar wind speed, density, and temperature, plasma beta, GMDN cosmic ray density, three components of the anisotropy, and the bubble plot of pitch angle distribution.

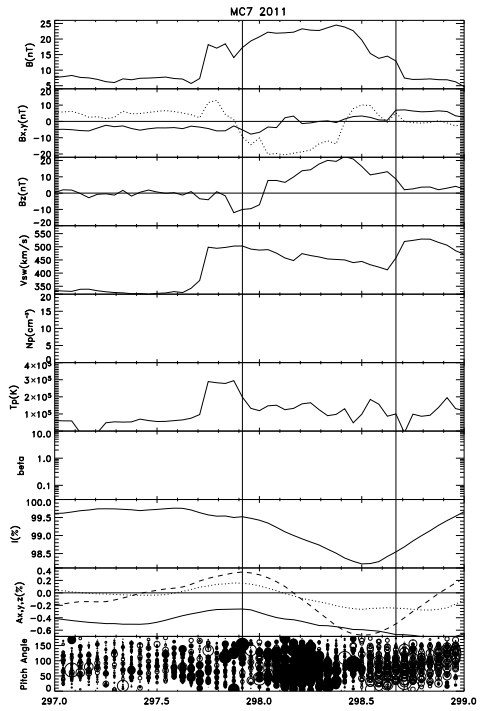

Fig. 2: Magnetic cloud occurred in October 24, 2011. From top to bottom we have the IMF intensity, the IMF components x and y, IMF z component, solar wind speed, density, and temperature, plasma beta, GMDN cosmic ray density, three components of the anisotropy, and the bubble plot of pitch angle distribution.

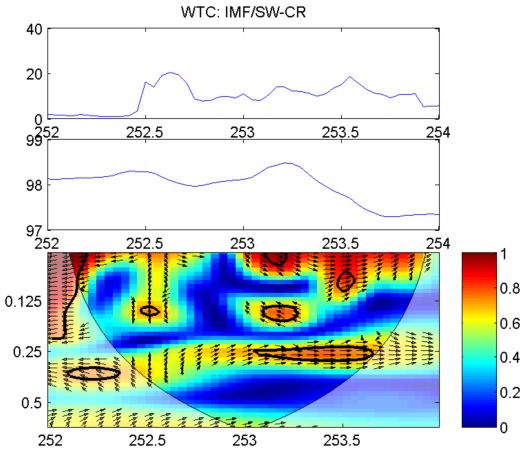

Fig. 3: Spectral coherence analysis (lower panel) between IMF intensity (top panel) and cosmic ray density (middle panel), for 11-MC4.

[4] C.P. Baker, M.L. Duldig, and J.E. Humble, Extensions to the coupling coefficient calculations for muon telescopes (1989), Proc. ASA, 8(1), 55-59.
[5] M.R. Silva, A. Dal Lago, W. D. Gonzalez, K. Munakata. C. Kato, J. Bieber, N. J. Schuch, M. L. Duldig, J. E. Humble, H.K. Al Jassar, M.M. Sharma and I. Sabbah, Geophysical Research Letters 38 (2011), doi:10.1029/2011GL048556.
[6] M.R. da Silva, D.B. Contreira, S. Monteiro, N.B. Trivedi, K. Munakata, T. Kuwabara and N.J. Schuch, Astrophysics and Space Science, 290 (2004) 389-397, doi:10.1023/B:ASTR.0000032537.23712.22.
[7] C.M.G. Lattes, G.P.S. Occhialini and C.F. Powell, Nature 160 (1947) 486-492 doi:10.1038/160486a0.
[8] M. Schönberg and S. Chandrasekhar, The Astrophysical Journal 96 (1942) 161-172 doi:10.1086/144444.
[9] A. Lara, N. Gopalswamy, R.A. Caballero-Lpez, S. Yashiro, H. Xie and J.F. Vlads-Galicia, The Astrophysical Journal (2005), 625:441-450, doi:10.1086/428565.
[10] H.V. Cane, Space Science Reviews (2000), v. 93, Issue 1/2, p. 55-77, doi:10.1023/A:1026532125747.
[11] R.P. Kane, Ann. Geophys. (2010), 28, 479489, doi:10.5194/angeo-28-479-2010.
[12] I.G. Richardson and H.V. Cane, Solar Physics 264 (2010) 189-237 doi: 10.1007/s11207-010-9568-6.
[13] I.G. Richardson and H.V. Cane, Solar Physics (2011) 270:609-627, doi: 10.1007/s11207-011-9774-x.
[14] R.K. Mishra and R. Agarwa, Brazilian Journal of Physics (2008), vol. 38, no. 4, December, doi:10.1590/S0103-97332008000500007.
[15] L.F. Burlaga, E. Sittler, F. Mariani, and R. Schwenn, Journal of Geophysical Research 6 (1981) 6673-6674 doi:10.1029/JA086iA08p06673.
[16] E. Echer, M. V. Alves and W. D. Gonzalez, Journal of Atmospheric and Solar-Terrestrial Physics 67 (2005) 839-852 doi:10.1016/j.jastp.2005.02.010.
[17] A. Grinsted, J.C. Moore and S. Jevrejeva, Nonlinear Proc (2004). Geoph., 11, 561-566, doi:10.5194/npg-11-561-2004.

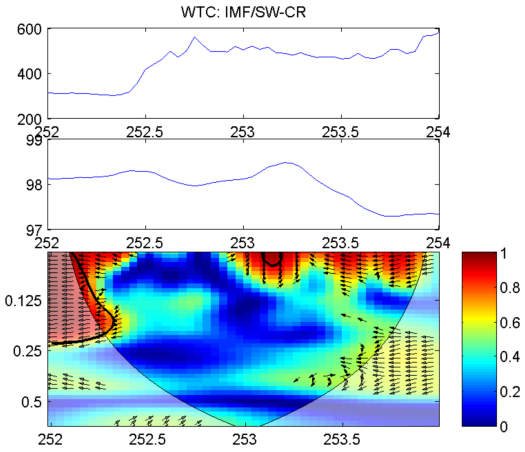

Fig. 4: Spectral coherence analysis (lower panel) between solar wind speed (top panel) and cosmic ray density (middle panel), for 11-MC4.

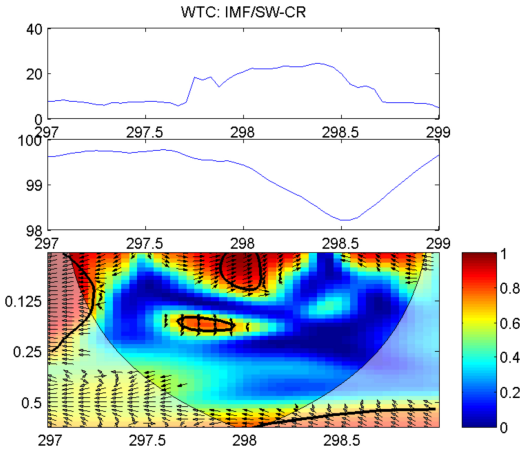

Fig. 5: Spectral coherence analysis (lower panel) between IMF intensity (top panel) and cosmic ray density (middle panel), for 11-MC7.

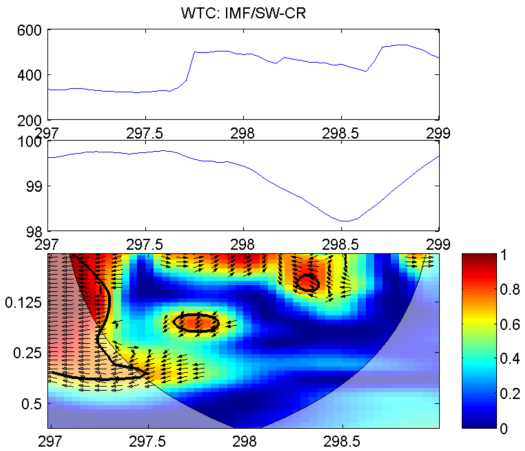

Fig. 6: Spectral coherence analysis (lower panel) between solar wind speed (top panel) and cosmic ray density (middle panel), for 11-MC7.